AMERICAN SCIENTIFIC PUBLISHERS

Journal of Nanoengineering and Nanomanufacturing
Vol. 1, pp. 18–34, 2011
(www.aspbs.com/jnan)

REVIEW

Recent Progress on the Superhydrophobic Surfaces with Special Adhesion: From Natural to Biomimetic to Functional

Yue-Kun Lai[1,2], Zhong Chen[2], and Chang-Jian Lin[1,*]

[1]*State Key Laboratory for Physical Chemistry of Solid Surfaces, and College of Chemistry and Chemical Engineering, Xiamen University, Xiamen 361005, China*
[2]*School of Materials Science and Engineering, Nanyang Technological University, 50 Nanyang Avenue, Singapore 639798, Singapore*

ABSTRACT

Superhydrophobic surfaces with drastically varying degree of liquid adhesions have attracted a lot of interest in both academia and in industry. In this review, recent progress of the natural superhydrophobic surface with varying solid–liquid adhesion strength has been reviewed, with a focus on the bio-inspired fabrication and application of such surfaces. Examples include lotus leaf inspired low adhesive surfaces, rose petal inspired high adhesive surfaces, biomimetic superhydrophobic surfaces with controllable and smart stimuli responsive liquid adhesion, and spider silk bio-inspired superhydrophobic surfaces with directional adhesion. In addition, we will review the significant applications related to artificial superhydrophobic structure surface with controllable adhesion. Finally, the challenges and prospects of this renascent and rapidly developing field are also briefly addressed and discussed.

KEYWORDS: Bio-Inspired, Wettability, Superhydrophobic, Adhesion, Application.

CONTENTS

*Author to whom correspondence should be addressed.
Email: cjlin@xmu.edu.cn
Received: 28 January 2011
Revised/Accepted: 12 March 2011

1. INTRODUCTION

In recent years, superhydrophobic surfaces, with a water contact angle (CA) greater than 150°, have attracted considerable interest due to their importance in both fundamental research and practical application.[1–15] Two types of extremely superhydrophobic cases exist in nature, which are the "sliding" superhydrophobic lotus leaves with ultralow water sliding resistance and the "sticky" superhydrophobic petal effect (and the gecko feet is another example) with high adhesive force. Biomimetic research indicates that the cooperation of morphological structures and chemical components plays a vital role on the special functional surfaces with varying adhesions. These findings have inspired the creation of superhydrophobic functional surfaces with self-cleaning, anti-icing/fogging, water/oil separation, micro-droplet manipulation, anti-bioadhesion, micro-template and low-friction transportation.[16–24]

In the following two sections, we will review the recent development (in the last three years) in the area of superhydrophobic surfaces with various water adhesions observed in nature, such as lotus leaf, mosquito eye, rose petal, spider silks, butterfly wings, gecko feet, desert beetle, and water strider (Fig. 1). The corresponding bio-inspired superhydrophobic surfaces with special wettability and solid–liquid adhesion are also reviewed

and discussed (superhydrophobic surface with weak/strong adhesion; superhydrophobic surfaces with anisotropic adhesion; and superhydrophobic surfaces with controllable/switchable adhesion). We will also review some significant applications related to superhydrophobic structure surfaces with special adhesion (Fig. 1). Finally, we briefly present our personal view on the problems and challenges encountered by the synthesis and practical application of the superhydrophobic surface with special solid–liquid adhesion.

2. SUPERHYDROPHOBIC SURFACES WITH SPECIAL WETTING STATES

Generally, compared with hydrophobic surfaces, artificial superhydrophobic surfaces exhibit apparent lower water adhesion. For example, typical superhydrophobic surface always has an average force approximately within 5–30 μN and a sliding angle smaller than 10°.[9] However, some superhydrophobic surfaces, under comparable contact angle, have displayed much stronger adhesion between the solid surface and the liquid. The interaction at the solid/liquid interface is ascribed to the contact modes and the details at the three-phase (liquid/air/solid) contact line (TCL). In the Cassie state, a great amount of air is trapped between the liquid/solid interface, the liquid/solid contact area is lower and the TCL is discontinuous.[25] Liquid droplets easily slide off due to the weak liquid/solid interaction. In contrast, at the Wenzel state a stronger liquid adhesion is displayed because the liquid fully penetrates and is in full contact with the solid surface, which has greatly increased the solid/liquid actual contact area. The corresponding TCL is continuous and stable.[26] Thus in this state, the surface generates relatively high adhesion, and liquid droplet does not fall off easily even after an external force is applied. However, in most cases, an intermediate state between Cassie and Wenzel states is always found due to the partial air trapped in the porous surface. Such an intermediate state is not stable and could be changed to the other contact state under external stimuli. This means water adhesion on such superhydrophobic surface can be adjusted and controlled without the change of solid surface

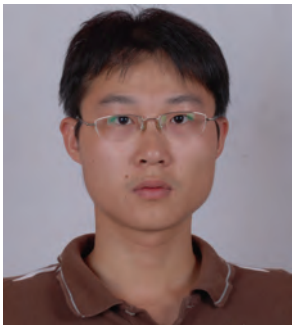

Yue-Kun Lai is currently working with Professor Harald Fuchs and Professor Lifeng Chi at Munster University, sponsored by the Germany Humboldt Foundation Scholarship. He received his B.S. degree in materials science from Fuzhou University, China in 2002. After that, he joined Professor Changjian Lin's group at Xiamen University and obtained his M.S. and Ph.D. degree in 2005 and 2009, respectively. Then, as a research fellow, he worked with Professor Zhong Chen at the School of Materials Science and Engineering, Nanyang Technological University (NTU), Singapore. His current scientific interests are focused on bio-inspired surfaces, intelligent materials, and functional composite patterns.

Zhong Chen is an Associate Professor at the School of Materials Science and Engineering, Nanyang Technological University (NTU), Singapore. He obtained his B.Eng., M.Eng., and Ph.D. degrees in 1984, 1987, and 1997 respectively. He joined NTU as a faculty member since March 2000. His current research interest focuses on thin films and nano-structures for electronics, clean energy, and environmental applications. Dr. Chen is an editor or member of the editorial board of 6 international academic journals, and has served as a reviewer for more than 40 journals. He has authored over 100 peer reviewed journal publications so far.

Chang-Jian Lin is a Distinguished Professor at the State Key Laboratory of Physical Chemistry of Solid Surfaces, Xiamen University, China. He obtained his B.S., M.S. and Ph.D. degrees in physical Chemistry in 1976, 1981 and 1985 respectively. He worked at National Institute of Standards and Technology (NIST) as a postdoctoral researcher from 1987–1990, and became a full professor since 1991 at Xiamen University. His current research interest focuses on materials electrochemistry, including corrosion and its research methods, biomaterials and surface nanoconstruction and nanostructures for energy and environment. Up to now, Dr. Lin has authored over 300 peer reviewed journal publications, and 45 patents.

REVIEW

Fig. 1. Some typical cases in natural (lotus leaf, mosquito eye, rose petal, spider silks, butterfly wings, gecko feet, desert beetle, and water strider) and their potential applications of bio-inspired superhydrophobic surfaces, such as self-cleaning, anti-icing/fogging, micro-droplet manipulation, fog/water collection, water/oil separation, anti-bioadhesion, micro-template for patterning, and friction-reduction.

morphologies and compositions. Accordingly, a series of solid/liquid adhesion strengths can be obtained through the manipulation of morphology and structure, surface composition and external stimuli. Therefore, Jiang et al. proposed five types of contact states on superhydrophobic surfaces according to their liquid adhesion form low to high as following: Lotus state; Cassie state; Intermediate state; Wenzel state and Gecko (petal) state.[27]

Normally, the liquid–solid adhesion is assessed by the sliding angle (contact angle hysteresis), which is defined as the difference between advancing and receding contact angles. The sliding angle on superhydrophobic surfaces can be influenced by the topography, structure, chemical heterogeneity, TCL, etc.[28–30] However, the measurement of sliding angle only indicates effects of adhesion along the shear direction. Moreover, it cannot quantitatively measure or even qualitative evaluated the adhesive force. For example, a water droplet will not roll away even if the high adhesive superhydrophobic surface is vertically tilted or turned upside down. To thoroughly understand the adhesion behavior between liquid and solid, the actual adhesive force should be also taken into account. To solve the problem, a high-sensitivity measurement system was developed by Professor Jiang et al. to quantitatively measure the real solid–liquid adhesion between the liquid droplet and the superhydrophobic surface: a liquid droplet is captured by superhydrophobic copper loop and suspended on the balance system, and the fixed surface on sample table is controlled to approach, contact and leave the droplet.[31] The maximum force required to take the droplet away from the surface is thought to be the adhesion between liquid and solid, which is related to the preload, the volume of droplet, etc. The sliding angle and actual adhesive force are two independent and complementary methods to characterize adhesion properties. In the following sections, various types of superhydrophobic surfaces with special adhesion are taken into account according to the practical case.

2.1. Superhydrophobic Surfaces with Weak Adhesion

In nature, many biological surfaces possess hierarchical micro- and nano-structures with low energy surfaces that provide the superhydrophobic properties with low water adhesion. Among them, the lotus leaves and water stride's legs are two typical examples (Fig. 2).[32–34] The phenomenon of effectively collecting the dirty debris along with the sliding of water droplets from the lotus leaf surface is commonly known as the "lotus effect". The lotus leaf therefore always keeps itself clean by this self-cleaning mechanism. Inspired by the self-cleaning effect of lotus leaves, various man-made superhydrophobic with low adhesion have been prepared by the construction of appropriate roughened structures with appropriate surface chemistry.[35–49]

Zhou and Liu et al. fabricate superhydrophobic metallic oxide layer on Ti and Al substrates by a simple combination of electrochemical anodizing and self-assembly technique.[35, 36] In comparison with the smooth surface, the nanoporous metallic oxide exhibited good self-cleaning performance and stability over a wide range of pH from acidic to alkaline. The good stability makes it possible for practical applications under various corrosive environmental conditions. Jiang's group successfully fabricated artificial water strider leg, using a water repellent material, which consists of a ribbed conical nanoneedle structure containing oriented nanogrooves sculptured on the lateral nanoneedle surface.[37] Such artificial leg exhibits good dynamic stability under loading and during load relaxation. In addition to the implication for the design of stable superhydrophobic structure surfaces, this work provides inspiration for the applications in drag-reduction materials and miniaturized aquatic robots/devices. Bhushan et al. prepared various self-cleaning functional superhydrophobic structures by replication of a micropatterned silicon surface using an epoxy resin and hydrophobic alkanes coating.[39–41] They also investigated the effect of lotus-like structures with various length scales on superhydrophobicity and self-cleaning efficiency. The important role of hierarchical structure for superhydrophobicity with low adhesion was revealed.

2.2. Superhydrophobic Surfaces with Strong Adhesion

In contrast to superhydrophobic surfaces with low adhesion, there are some other surfaces (rose petals and gecko

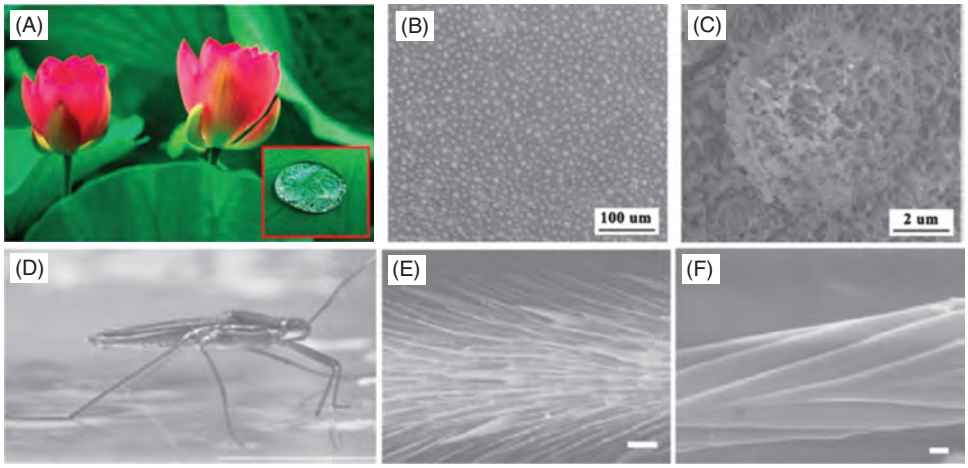

Fig. 2. (A) Superhydrophobic lotus leaf and water droplet on the leaf (inset). (B) Low magnification scanning electron microscope (SEM) image of the surface structures on the lotus leaf. (C) High-resolution SEM (HRSEM) image of a single papilla consisting of cilium-like nanostructures. Reprinted with permission from Ref. [32], K. S. Liu et al., *Appl. Phys. Lett.* 92, 183103 **(2008)**. © 2008, American Institute of Physics. (D) A water strider standing on a water surface with its long legs. (E, F) The two-level hierarchical structure of a water strider's leg1 exhibits microsetae (bar = 20 μm) with fine nanoscale grooves (bar = 200 nm). Reprinted with permission from Ref. [33], X. F. Gao and L. Jiang, *Nature* 432, 36 **(2004)**. © 2004, Nature Publishing Group.

toes) on which water droplets are firmly pinned to the surface but at the same time keep a large (more than 150°) static contact angle.[50–53] To illustrate the origin of this high adhesive force, Feng et al. studied the microstructures of rose petal.[50] Figure 3(A) exhibits that the rose petal surfaces are composed of a periodic array of micro-papillae with compactly arranged structures. Moreover, nanoscaled cuticular folds are found on the top of the micro-papillaes (Fig. 3(B)). Water droplets are expected to penetrate into the microscale papillae, but air trapped inside the nanoscale folds, therefore forming Petal-state with strong adhesion. To confirm such special dual-scale structures, they used polystyrene (PS) and polydimethylsiloxane (PDMS) to directly duplicate the structures of rose petals and found that the artificial petal-like structure surface do possess superhydrophobic property with a strong water adhesion.

Recently, several attempts have been made to fabricate sticky superhydrophobic surfaces, on which a water droplet does not roll off even with a 180 degree tilt.[54–60] Jin and co-workers successfully prepared well-ordered superhydrophobic polystyrene nanotubes with high hysteresis by using alumina membrane templates.[31] They believed the key factor responsible for the great adhesion is the enhancement of van der Waals forces between the densely packed nonpolar polystyrene nanotubes in close contact with water. Guo et al. reported a simple and inexpensive method to fabricate a sticky superhydrophobic surface via etching of an aluminum alloy surface and eliminating its loose layer.[55] They subsequently demonstrated that an even-stronger adhesion is achievable due to the joint action of capillary forces and van der Waals forces from the micro-orifices and hydrophilic nanoparticle composite structures, respectively.

2.3. Superhydrophobic Surfaces with Controllable Adhesion

2.3.1. Topography and Structure

From the theoretical background of special wetting states, it is easy to understand that the morphological and structural parameters are vital to influence the adhesion of a droplet on superhydrophobic surfaces. For the same material, the solid/liquid adhesion can be effectively controlled by tailoring the morphology or the scale of the structures on the surface.[61–70] There are many techniques to construct superhydrophobic surface with different morphologies and structures, for example by electrochemical anodizing, dry/wet etching, phase separation and thermal treatment.

Recently, we designed and successfully fabricated three types of superhydrophobic nanostructure models consisting of a nanopore array (NPA), a nanotube array (NTA), and a nanovesuvianite structure (NVS) by electrochemical anodization (Fig 4).[61] These various structures could tune the wetting states and air-pocket ratio in sealed and open systems, so that the solid/liquid adhesion could be effectively controlled in a wide range. Capillary adhesive force plays a dominant role in imparting adhesive behavior on NPA and NTA nanostructures due to the formation of sealed air pockets, while the NVS nanostructures exhibit extremely low adhesion due to the absence of closed air pockets. In addition, adhesive forces could be tuned by changing the nanotube diameter, especially by nanotube length, due to negative pressure caused by the volume change of air sealed in the nanotubes. These findings are valuable to deepen insight into the roles of nanostructures in tailoring surface water-repellent and adhesive properties for exploring new applications. Similarly, Lee et al. also

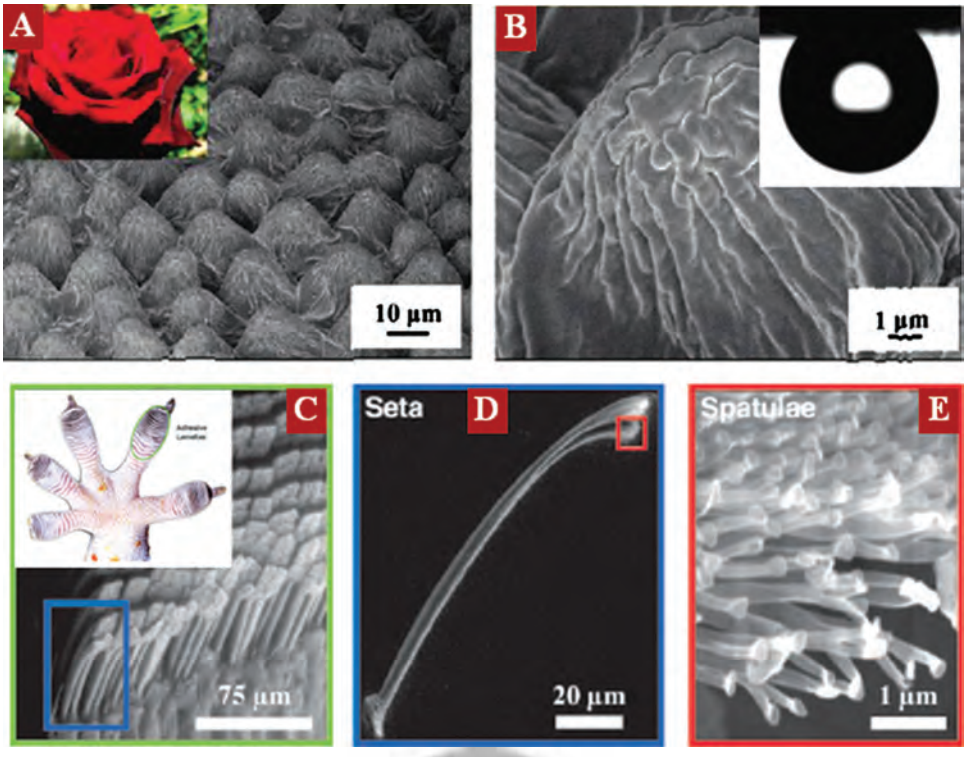

Fig. 3. (A) SEM images of the surface of a red rose petal, showing a periodic array of micropapillae and (B) nanofolds on each papillae. Inset: Shape of water on the petal's surface when it is turned upside down. Reprinted with permission from Ref. [50], L. Feng et al., *Langmuir* 24, 4114 **(2008)**. © 2008, American Chemical Society. (C) Microfeatures of a gecko toe surface: proximal portion of a single lamella, with individual setae in an array visible. Inset: Ventral view of the foot, with adhesive lamellae (scansors) visible as overlapping pads. Note the clean appearance of the adhesive surface. (D and E) Nanostructure: single seta with branched structure at upper right, terminating in hundreds of spatular tips. Reprinted with permission from Ref. [52], K. Autumn et al., *Nature* 405, 681 **(2000)**. © 2000, Nature Publishing Group.

reported the adhesiveness-controllable superhydrophobic anodized aluminum oxide (AAO) by tuning the structure with the formation ratio of dead-end nanopores.[62,63] With increasing of dead-end nanopore ratio, the decrease in the receding angle and an increase in the hysteresis of water contact angles.

2.3.2. Chemical Composition

The chemical component is another important factor in determining the surface contact angle and solid/liquid adhesion. For a superhydrophobic surface with identical morphology, the solid/liquid adhesion could be greatly controlled by adjusting the ratio of high energy hydrophilic component.[71–77] Recently, we presented a successful example of the superhydrophobic spongy-like TiO_2 surface exhibiting water adhesion ranging from ultralow (5.0 μN) to very high (76.6 μN) by adjusting the nitrocellulose (NC) dosage concentrations in 1*H*,1*H*,2*H*,2*H*-perfluorooctyltriethoxysilane (PTES) methanol solution (Fig. 5).[72] The superhydrophobic samples without the introduction of NC showed an ultralow adhesion with a sliding angle about 0.8°. The film after NC-PTES mixed modification can hold a water droplet even when it is turned upside down, indicating a high adhesive force to droplet. The significant increase of adhesion by introducing nitrocellulose was ascribed to the fact that the hydrophilic nitro groups, which not only lead to the disruption of the densely packed hydrophobic PTES molecule but also result in the formation of hydrogen bonding with the hydroxyl groups at the solid/liquid interfaces.

Another example is area selective removal of low surface energy materials on rough structures to obtain patterned surface with micrometer-scale chemically heterogeneous composition.[78,79] Zhou's group realized tunable water adhesion by adjusting the amounts of amphiphilic molecules domains on the superhydrophobic surfaces.[80] Although the resultant surfaces showed superhydrophobic behavior without obvious contact angle decrease, the adhesion was greatly enhanced. These findings are helpful to effectively fabricate novel functional nanomaterials with customer-tailored surface hydrophobicity and adhesion by uniformly modifying the rough surface with various concentrations of high surface energy materials or by creating chemically heterogeneous composition.

2.4. Superhydrophobic Surfaces with Responsive Adhesion

Most cases reported so far deal with controllable, rather than responsive and switchable adhesion by manipulating

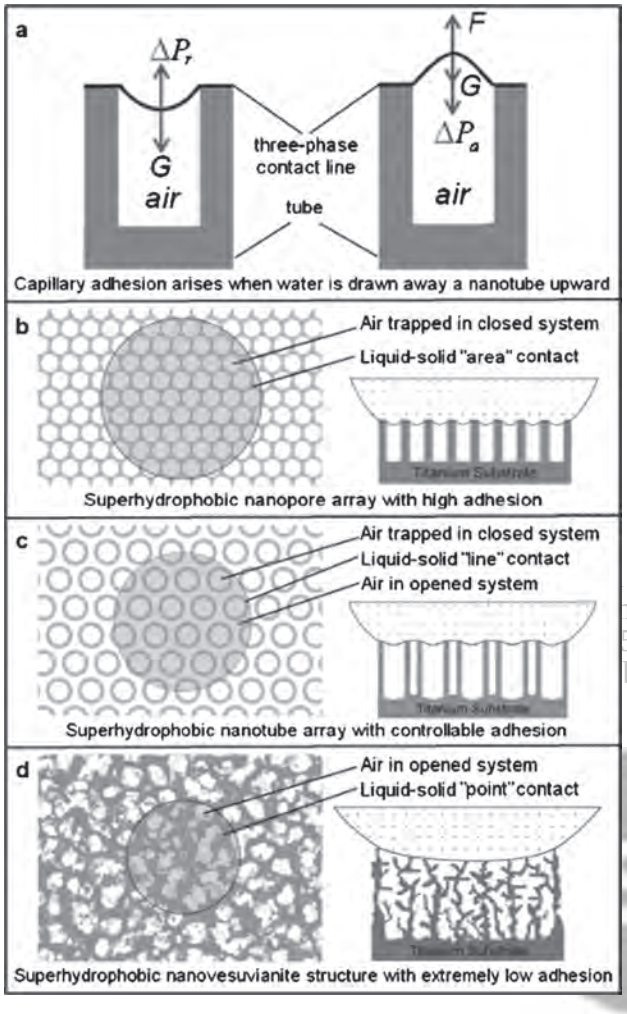

Fig. 4. Schematic illustration of three types of superhydrophobic porous-nanostructure models with different adhesion. (a) Schematic illustration of NPA caused by negative pressure when a water droplet is drawn away; (b) Superhydrophobic NPA with high adhesion; (c) Superhydrophobic NTA with controllable adhesion; (d) Superhydrophobic NVS with extremely low adhesion. Reprinted with permission from Ref. [61], Y. K. Lai et al., *Adv. Mater.* 21, 3799 **(2009)**. © 2009, Wiley-VCH Verlag GmbH & Co. KGaA.

the solid–liquid contact mode or by adding hydrophilic molecules onto the superhydrophobic background. The change in the contact angle hysteresis (decreasing of the receding angle) is a key factor to control droplet mobility on surfaces. It is well known that the solid/liquid adhesion on superhydrophobic surface is greatly dependent on the wetting state. In general, a Cassie-state superhydrophobic surface exhibits lower adhesion to liquid droplets, while the adhesion will be dramatically enhanced for a Wenzel wetting state surface. There exist energy barriers to prevent the spontaneous transition between the Wenzel and Cassie states. If an external stimulus (e.g., photo,[81–83] electricity,[84–88] temperature,[89,90] magnetic field,[91,92] transformation,[93,94] pH,[95] and multi-responsive factors[96–98]) can be applied to induce the transition, the adhesion will be reversibly switched. In recent years, smart wettability responsive surfaces with reversibly switching between superhydrophilicity and superhydrophobicity have attracted increasing interests.

Among the photo-responsive materials, azobenzene and its derivatives are known to exhibit changes in under UV/visible irradiation because of its reversible photoisomerization between the cis- and trans-conformations. Liu and coworkers reported that water droplet mobility can be reversibly manipulated by using a photo-responsive azobenzene and polydimethylsiloxane coated on a rough anodized alumina surface.[81] The surface coating consists of silicone elastomer as the basic hydrophobic material and the incorporated azobenzene compound as photosensitizer that assumes trans-/cis-conformation change under visible and UV illumination (Fig. 6). The surface thus could switch between sliding and sticky states when the azo-compound assumes trans- and cis-conformation, while the contact angle on the superhydrophobic surface doesn't change apparently.

Krupenkin et al. demonstrated for the first time the dynamic electrical control over the liquid droplets on superhydrophobic nanostructured surfaces by etching microscopic array of cylindrical nanoposts into the surface of a silicon wafer, finding that the electrowetting properties of the surface can be tuned from superhydrophobic behavior to nearly complete wetting as a function of applied voltage and liquid surface tension.[84] Zhao et al. reported a superhydrophobic membrane of MnO_2 nanotube arrays on which water adhesion can be adjusted by applying a small DC bias.[85] For a 3 μL water droplet, the measured adhesive force increased and reached a maximum of 130 μN at a negative voltage of 22 V, which was 25 times higher than that of the original value before the introduction of the electrical field. Moreover, the electrically adjustable adhesion is strongly polarity-dependent: only a five-fold increase is found when a positive bias of 22 V is applied. This remarkable electrically-controlled adhesive property is ascribed to the change in contact geometry between the water droplet and MnO_2 nanotube array, on which water droplets exhibit the different continuities of three-phase contact line. Recently, Liu et al. developed an *in situ* oil adhesive force measurement in an oil/water/solid system. When the polypyrrole film was oxidized, the oil adhesive force measurement was about 8.7 μN. In contrast, a lower oil adhesion about 1.6 μN was found on the reduced state polypyrrole film.[86]

Li et al. reported a thermal stimuli responsive surface by simply spin-coating a side-chain liquid crystal polymer, PDMS-4OCB, on an optimized rough silicon wafer.[89] Reversible switch of the mobility of a water micro-droplet between rollable and pinned states is realized simply by changing the temperature. The change had caused the phase transition of a side-chain liquid-crystal polymer with optimized surface roughness in a superhydrophobic

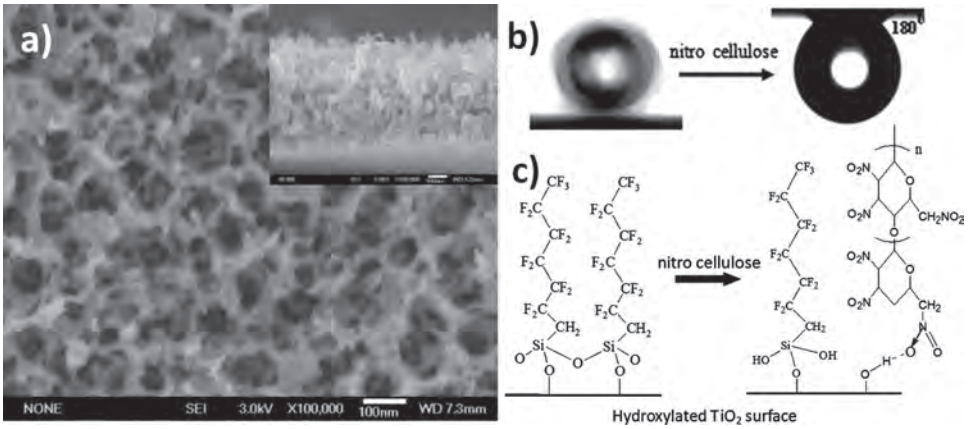

Fig. 5. (a) Top-view SEM image of a typical sponge-like structure TiO_2 film on titanium substrate. The inset shows the cross-sectional SEM image. (b) Behavior of a water droplet on sponge-like TiO_2 surface before and after NC introduction. (c) Model of molecular self-assembly before and after NC introduction. Reprinted with permission from Ref. [72], Y. K. Lai et al., *Langmuir* 24, 3867 **(2008)**. © 2008, American Chemical Society.

surface. Jiang's group reported a superhydrophobic iron surface that had a tunable adhesive force with the superparamagnetic microdroplet as a function of the magnetic field. Reversible transition between the high adhesion and low adhesion can be achieved by simply magnetizing and demagnetizing the surface alternately.[91, 92]

2.5. Superhydrophobic Surfaces with Anisotropic Adhesion

If a textured surface shows different contact angles or sliding angles when measured in various directions, the surface is said to be anisotropic in wettability, otherwise it is isotropic. Recent studies revealed that anisotropic adhesion was attributed to the anisotropic three-phase contact line.[100, 101] For example, butterfly wings have directional adhesion.[102] A water droplet can easily roll off the surface of wings along the radial outward direction of the central axis of the butterfly body, but it is firmly pinned in the opposite direction. It is demonstrated that this unique ability is ascribed to the direction-dependent arrangement of the flexible nanotips and microscales on the wing resulting in the great change of the TCL in different directions. When the wing is tilted down, the oriented nanotips separate from each other to form a discontinuous TCL, which makes the droplet easily roll off the wing surface. In the case of wing tilted upward, the flexible nanotips and microscales take a close arrangement to form a quasi-continuous TCL, which pins the droplet on the wing.

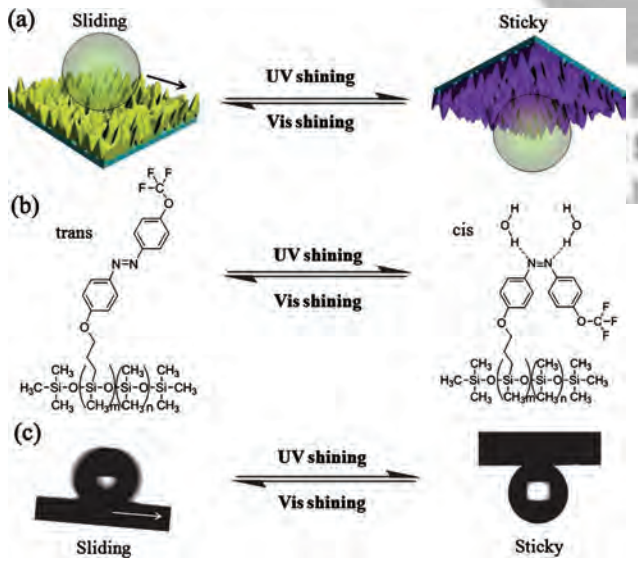

Fig. 6. (a) Schematic illustration of the mechanism of water droplet reversible adhesion on polydimethylsiloxane and azobenzene modified anodized alumina upon UV and vis irradiation; (b) the trans and cis molecular structure transformation of azo groups by UV and vis irradiation; (c) photographs of water droplet switchable adhesion on polydimethylsiloxane kits and azobenzene (same ratio) modified anodized alumina under photo-switchable irradiation. Reprinted with permission from Ref. [81], X. J. Liu et al., *Soft Matter* DOI: 10.1039/c0sm01144d **(2011)**. © 2011, The Royal Society of Chemistry.

Anisotropic superhydrophobic surfaces allow butterflies to shed off water from their wings, spider silk to collect water, and plants to trap insects and pollen. Anisotropic wetting surfaces have attracted a great amount of attention due to their advantage in many potential applications in microfluidic devices, and self-assembled pattern formation. Recently, Demirel et al. reported an engineered nanofilm, composed of an array of poly(p-xylylene) nanorods (Fig. 7), which demonstrates anisotropic wetting behavior by means of a pin-release droplet ratchet mechanism.[103] Droplet retention forces in the pin and release directions differ by up to 80 μN, which is much higher than the values reported for other engineered anisotropic surfaces. The nanofilm provides a microscale smooth surface on which microlitre droplets are transported. It is also relatively easy to synthesize such structures by a bottom-up vapor-phase technique. Inspired by butterfly wings, Yeomans et al. investigated the equilibrium behavior and dynamics of droplets on a superhydrophobic surface with patterned sawtooth or posts.[104] They also found the both partially suspended and collapsed

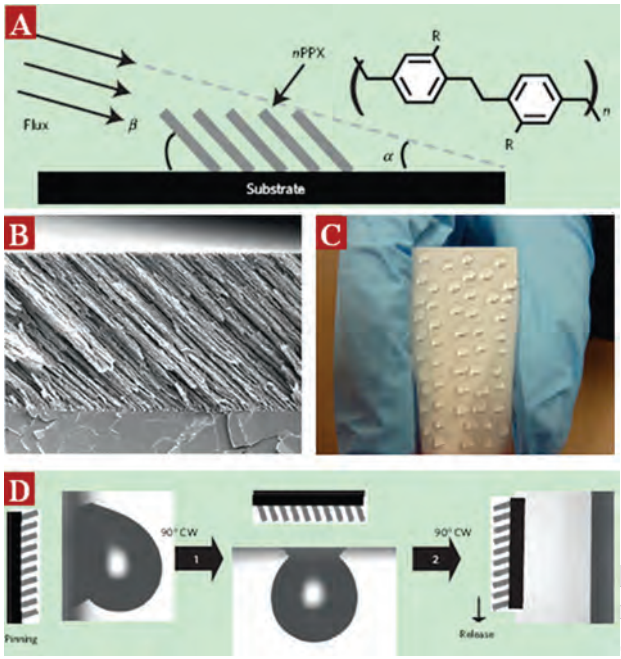

Fig. 7. An overview of poly(p-xylylene) nanofilm preparation and anisotropic wetting property. (A) Schematic of poly(p-xylylene) nanofilm deposition by oblique angle polymerization; (B) Electron microscope cross-section of poly(p-xylylene) nanofilm; (C) Picture of the anisotropic adhesive wetting surface with water drops; (D) Water adhesion and release in three configurations of the nanofilm. Schematics illustrate the nanorod inclination at different tilt angle and correspond to photographs showing the anisotropic wetting behavior of the nanofilm. Reprinted with permission from Ref. [103], N. A. Malvadkar et al., *Nat. Mater.* 9, 1023 **(2010)**. © 2010, Nature Publishing Group.

configurations have large anisotropic response to an external force.

3. APPLICATIONS OF SUPERHYDROPHOBIC SURFACES WITH SPECIAL ADHESION

While the biomimetic superhydrophobic surfaces with special adhesion have been fabricated by various methods as discussed above, attention has also been shifted to the functional applications in the recent a few years. Many important applications, such as self-cleaning,[106–111] anti-icing/fogging,[112–121] micro-droplet manipulation,[31, 91–93, 122–126] fog/water collection,[127–133] water/oil separation,[134–140] anti-bioadhesion,[141–150] micro-template for patterning,[161–170] and friction reduction[172–181] could be realized through the improved understanding of superhydrophobicity with varying degree of adhesion. Selected examples are discussed below.

3.1. Self-Cleaning

Surface self-cleaning is a significant application of superhydrophobic surface, typically by the lotus leaf.[105] For a drop of water rolling off a lotus leaf, the droplet behaves as an elastic ball rather than a fluid. In case of a normal hydrophobic surface, because of the nonslip boundary condition, the water drop falls across the dirt particles and the dirt particles are mainly displaced to the sides of the droplet and re-deposited behind the droplet. Especially hydrophobic particles tend to remain on such surfaces (Fig. 8(a)). In the case of superhydrophobic rough surfaces, the solid/water interface is minimized. Water forms a spherical droplet and easily rolls off, and the droplet collects the particles from the surface (Fig. 8(b)). Therefore, the superhydrophobic rough surfaces with low adhesion always exhibit a very low degree of contamination, which is what known as self-cleaning.[106–111] Barthlott et al. investigated the wetting and the self-cleaning properties of three types of superhydrophobic surfaces: hydrophobized silicon spike array surface, replicates of water-repellent leaves of plants, and fluorinated commercially metal foils.[106] When only subjected to artificial fog, metal foils and some replicated surfaces have lower clean efficiency than the silicon surfaces. This is due to their two-level rough structures in which dust cannot be caught by the droplets. In the case of water drops impinging with sufficient kinetic energy, all superhydrophobic surfaces could be cleaned perfectly.

3.2. Anti-Icing/Fogging

Ice or wet snow adhesion and accretion on solid materials, especially power lines and transportation vehicles in some cold regions, may lead to severe damages. Most current deicing systems employ either physical or chemical method to remove of ice after its formation, and they cost energy and resources dearly. Recently much attention has been given to study the freezing of static water droplets resting on super-cooled surfaces. Ice accretion, however, begins with the droplet/substrate collision

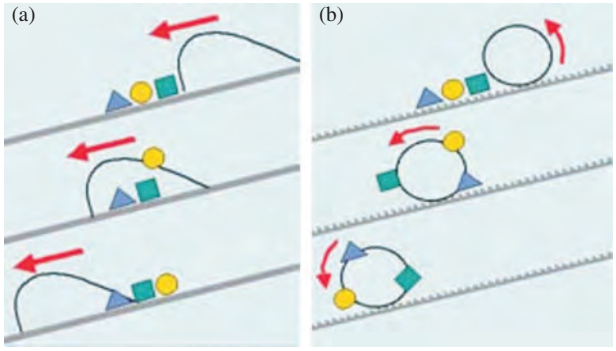

Fig. 8. Slip of a water droplet from an inclined hydrophobic surface (a) where the water drop crawls over the dust particles and an inclined superhydrophobic surface (b) where the dust particles are collected and taken away in a self-cleaning process. Reprinted with permission from Ref. [105], W. Barthlott and C. Neinhuis, *Planta* 202, 1 **(1997)**. © 1997, Springer.

followed by freezing. Pre-emptive deicing, which prevents ice formation or reduce ice adhesion and accumulation rather than to fight its build-up is of greater interest. Aizenberg and coworkers studied the behavior of dynamic droplets impacting super-cooled surfaces with superhydrophobicity.[112] It showed that highly ordered superhydrophobic materials could be designed to remain entirely ice-free down to ca. −25 to −30 °C, due to their ability to repel impacting water before ice nucleation occurs. Ice accumulated below these temperatures can be easily removed. A stream of droplets ($T_{droplet} = 0$ °C) was dropped from a 10 cm height at a rate of 0.06 mL/sec onto various surfaces (flat aluminum, smooth fluorinated silicon, and microstructured fluorinated silicon) with different contact angles onto a 30° tilted substrate at −10 °C. While the flat hydrophobic surface showed a ∼1 min delay in ice formation as compared to the hydrophilic surface, both surfaces were found significant ice accumulation after 10 min (Figs. 9(A, B)). The latter observation suggests that surface chemistry alone is of limited help in ice-prevention technologies, as it could only delay but not avoid ice buildup. The superhydrophobic surface, on the other hand, is a promising alternative, as no ice accumulation was observed after 10 min of water flow (Fig. 9(C)). Kulinich et al. studied the adhesion strength of artificially created glaze ice on rough fluoropolymer-based superhydrophobic surface with different CA and wetting hysteresis, showing that the ice adhesion strength on rough hydrophobic surface has no correlation with water CA, but has good correlation with wetting hysteresis.[113] Gao et al. demonstrated the anti-icing capability of superhydrophobic surfaces using nanoparticles and polymer composites. It was able to prevent ice formation upon impact of super-cooled water both in laboratory conditions and in natural environments.[114] They found that the anti-icing capability of these composites depends not only on high wettability but also on the size of the particles (roughness) exposed on the surface. In fact, icing of supercooled water on superhydrophobic surfaces is a complex phenomenon, which can be affected by multiple factors including the temperature, real contact area, surface chemistry, and roughness.

Besides the good anti-icing performance, superhydrophobic surfaces can also retard frost formation due to the metastable state of the three-phase line, compared with that on a smooth hydrophobic surface.[115–119] Gao et al. found the superhydrophobic compound eyes of mosquito are comprised of the smart design of elaborate micro- and nanostructures: nanoscale of hexagonally non-close-packed nipples and microscale of hexagonally close-packed ommatidia.[116] Such ideal composite structures can efficiently prevent fog drops from condensing and being trapped on the superhydrophobic surface to provide an effective protective mechanism for maintaining clear vision under environmentally humid condition. They also successfully fabricated artificial superhydrophobic compound eyes with good anti-fogging performance by employing soft lithography methods to transfer polydimethylsiloxane micro-hemispheres and silica nanospheres. The easy rolling of water or fog droplets may take the dust particles away from the superhydrophobic compound eye-like surface with a low adhesive force, thereby achieving self-cleaning and anti-fogging in a humid habitat. Very recently, He et al. reported the uniform ZnO nanorod array surfaces kept superhydrophobic not only to sessile macro-droplets at room temperature but also to condensed micro-droplets at temperatures below the freezing point (−5 °C or −10 °C).[119] The time of condensed droplets maintaining the liquid state (retardation period) increases with the increasing of contact angle on the superhydrophobic ZnO surfaces, indicating an obvious retardation and prevention of ice/frost formation. In general, the study of the anti-icing and anti-fogging of superhydrophobic surfaces is just at its beginning stage.[116, 120, 121] Further research is needed to understand the controlling factors to achieve optimized performance.

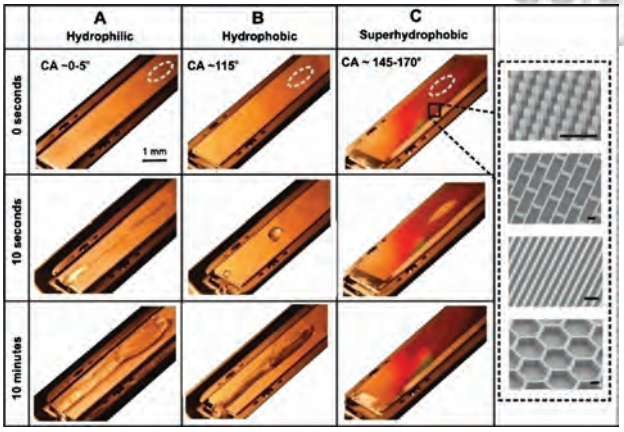

Fig. 9. Ice accumulation on flat aluminum (A), smooth fluorinated Si (B), and microstructured fluorinated Si (C) surfaces. The advancing contact angle of the water droplets on these surfaces is indicated. Insets show micrographs of exemplary superhydrophobic surfaces: posts, bricks, blades, and honeycombs (scale bars: 10 μm). White dashed circles indicate the position of droplet impact. Reprinted with permission from Ref. [112], L. Mishchenko et al., *ACS Nano* 4, 7699 (**2010**). © 2010, American Chemical Society.

3.3. Micro-Droplet Manipulation

The efficient manipulation of low-volume droplets offers many potential applications in relation to chemical and biomedical tests and protocols. Superhydrophobic surfaces with controllable/responsive adhesion in a high contrast show attractive application in micro-droplet manipulation.[122–126] Hence, efforts have also been devoted to improve the transferring process. For example, Jin *et al.* prepared high adhesive superhydrophobic polystyrene nanotube surfaces and used them to catch micro-droplet

from low adhesive superhydrophobic surface. The droplet was then released to a hydrophobic/hydrophilic target.[31] Following this work, they further reported an *in-situ* control and transfer of magnetic droplet movement using magnetic field.[91,92] Recently, Sun and Jiang et al. reported a more practical and facile technique to transfer a water droplet by the deformation-induced reversible adhesion transition on superhydrophobic polydimethylsiloxane surface.[93] They changed the surface curvature to adjust water droplet adhesion on polydimethylsiloxane pillar array surface from a highly adhesive "pinned" state to a low adhesive "roll-down" state. This provides the possibility for precise, no-loss transportation of water droplets. Furthermore, Breedveld et al. reported the facile high surface energy black ink patterning on superhydrophobic paper substrates by using commercially available desktop printing technology.[122] The tunability of the superhydrophobic surface adhesion was used to implement four basic operations for the manipulation of liquid drops on the paper substrates from storage, transfer, mixing to sampling (Fig. 10). In their two-dimensional lab-on-paper prototype, liquid droplets adhere to the porous substrate, rather than absorbing into the paper; as a result, liquid droplets remain accessible for further quantitative testing and analysis after performing simple qualitative on-chip testing.

3.4. Fog/Water-Collection

In many countries, the mornings in spring are graced with spectacular displays of dew drops hanging on spiders' webs and on leaves.[127–129] Some leaves, in particular, spot particularly large droplets that last well into the morning. Recently, Zheng et al. fully investigated the detailed mechanistic insights into directional water collection on spider silk.[127,128] They found that the structure of spider silk took place a 'wet-rebuilt' change to periodic spindle-knots made of random nanofibrils and separated by joints made of aligned nanofibrils after wetting. Guided by the spider silk, they successfully fabricated artificial fibre that not only mimics the structure of wet-rebuilt spider silk but also its directional water collection capability (Figs. 11(A, B)).

Another example lies with some beetles in the water limited Namib Desert who collect drinking water from fog-laden wind on their backs.[130–133] Large droplets form by virtue of the insect's bumpy surface which consists of alternating wax-coated hydrophobic and non-waxy hydrophilic regions. Inspired by the water collecting structure of the desert beetle's back, Cohen et al. fabricated hydrophilic or superhydrophobic patterns on superhydrophobic surfaces with similar fog-collecting characteristics with desert beetle (Figs. 11(C, D)).[131] Hydrophilic patterns on superhydrophobic surfaces were created with water/2-propanol solutions of a polyelectrolyte to produce surfaces with extreme hydrophobic contrast. Selective deposition of multilayered films onto the hydrophilic patterns introduces different properties to the area.

3.5. Water/Oil Separation

Water/oil separation technology is very important for a wide range of environmental, biomedical, agricultural, and industrial applications.[134–140] Technically, the separation can be achieved by selective liquid adhesion/permeation. The separation of oil from oil contaminated water is considered as a difficult task due to some well-known problems associated with the present systems, including low separation efficiency and involvement of complex separation instrument. The use of separation membrane with high wetting contrast could provide a low cost, high efficiency solution. In recent years, researchers started exploring the use of superhydrophobic and superoleophilic films or powers for separation of oil from water in the mixture.[134–136] Different materials and processes have been investigated. For example, Feng et al. firstly reported the water/oil separation by using the superhydrophobic and superoleophilic mesh. They coated hydrophobic PTFE on stainless steel mesh by spray-and-dry method.[137] The prepared mesh exhibit a kind of micro- and nanocomposite structure.

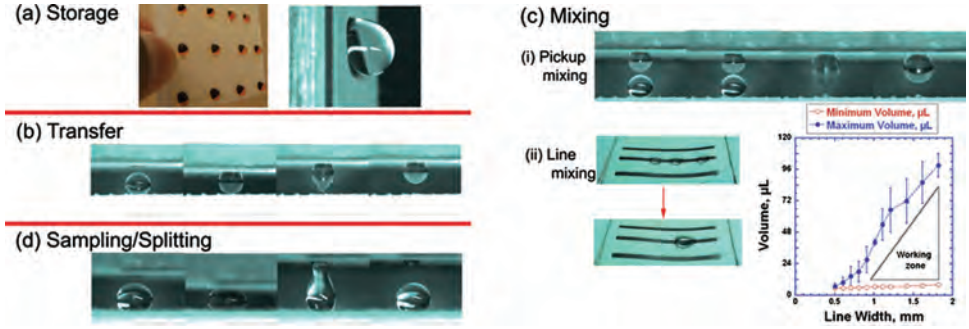

Fig. 10. (a) Photographs of an array of drops (food coloring was added to enhance contrast) and a high magnification image of a single drop stored on a vertical substrate, (b) a series of snapshots of a drop being transferred between two substrates, (c) photographs of merging and mixing: (i) via "pickup mixing" (two drops), (ii) "line mixing" (three drops) and plot that shows the working zone of drop volumes suitable for line mixing, (d) photographs of drop splitting between two substrates. Reprinted with permission from Ref. [122], B. Balu et al., *Lab Chip* 9, 3066 **(2009)**. © 2009, The Royal Society of Chemistry.

REVIEW

REVIEW

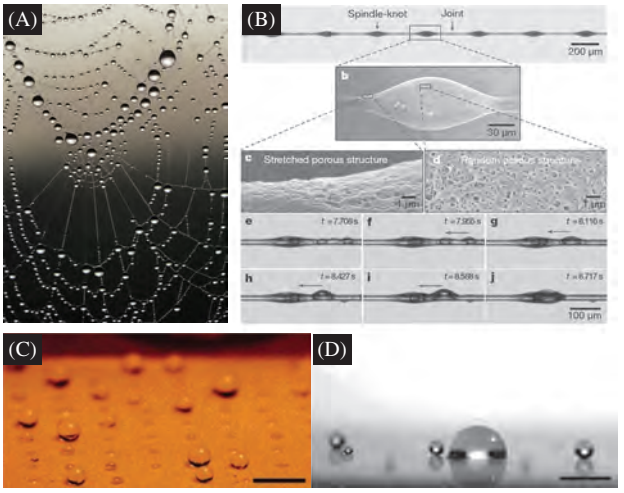

Fig. 11. (A, B) Spider silk and bio-inspired artificial fibre with directional water adhesion. Reprinted with permission from Ref. [127], Y. M. Zheng et al., *Nature* 463, 640 **(2010)**. © 2010, Nature Publishing Group. (C) Small water droplets sprayed on a (PAA/PAH/Silica nanoparticle/semi-fluorosilane) superhydrophobic surface with an array of hydrophilic domains patterned with a 1% PAA water/2-propanol solution; (D) Sprayed small water droplets accumulate on the patterned hydrophilic area shown in (C). Reprinted with permission from Ref. [131], L. Zhai et al., *Nano Lett.* 6, 1213 **(2006)**. © 2006, American Chemical Society.

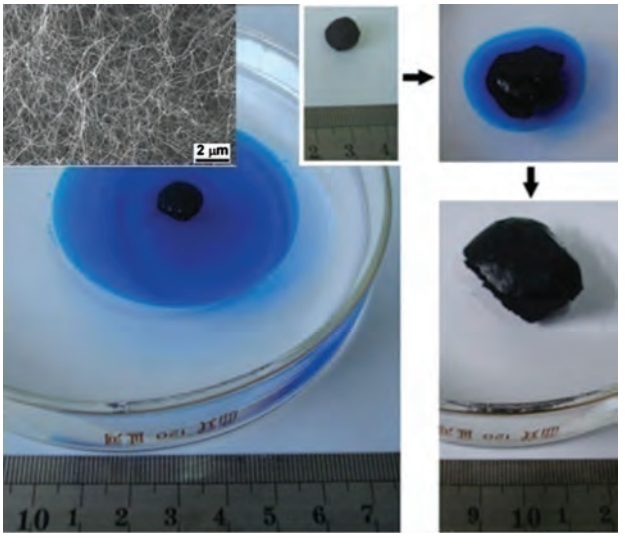

Fig. 12. Snapshots showing the absorption of a 28 cm^2 and mm-thick vegetable oil film (dyed with Oil Blue) distributed on a water bath by a small spherical sponge. Inset: SEM image of the as-prepared three-dimensional random interconnected carbon spongy. The growing size of the sponge accompanied by the shrinkage of oil film indicates continuous oil absorption and storage inside the sponge. Reprinted with permission from Ref. [140], X. C. Gui et al., *Adv. Mater.* 22, 617 **(2010)**. © 2010, Wiley-VCH Verlag GmbH & Co. KGaA.

Diesel oil droplet could spread and permeate through the mesh within only 240 ms, indicating superoleophilic, while water droplet shows spherical shape with a contact angle of 156.2°. Zhang et al. prepared composite film composed of porous polyurethane and polystyrene microspheres to enhance the hydrophobicity and oleophilicity of the surface.[138] However, among these approaches and materials used, the fabrication process usually was time-consuming, and wettability contrast may degrade under harsh and corrosive environment. These drawbacks have limited their practical application. Therefore, exploration into more stable material with simple preparation process is highly desirable to produce filtering membranes that exhibit simultaneous superhydrophobic and superoleophilic properties. Another important water/oil separation process is the preparation of high porous membranes with superoleophilic that can fast absorb oil with high absorption capacity. Kong and Stellacci et al. presented a self-assembly method for constructing thermally stable, free-standing nanowire membranes that exhibit controlled wetting behavior ranging from superhydrophilic to superhydrophobic.[139] These membranes can selectively absorb oils up to 20 times the material's weight in preference to water, through a combination of superhydrophobicity and capillary action. Moreover, the nanowires that form the membrane structure can be re-suspended in solutions and subsequently re-form the original paper-like morphology over many cycles. Their results suggest an innovative material that may find practical applications in the removal of organics, particularly in the field of oil spill cleanup. Recently, Cao et al. reported a three-dimensionally interconnected hydrophobic carbon nantube sponges by chemical vapor deposition. They can absorb many kind of solvents and oils with excellent selectivity, recyclability and absorption capacities up to 180 times to their own weigh (Fig. 12).[140] A small densified spongy floating on water can rapidly uptake a spreading oil film with an area up to 800 times than that of the spongy.

3.6. Anti-Bioadhesion

Many factors, such as composition, topography, charge and wettability, are vital in the surface conditions for biological applications. Surface with unique wettability is one of the most important factors influencing protein adsorption, platelet adhesion, bacteria adhesion and cell culture.[141–150] Wall adsorption is a common problem in microfluidic devices, particularly when proteins are involved. Recently, Shirtcliffe and coworkers show that superhydrophobic surfaces can be used to reduce protein adsorption and to promote desorption.[141] Hydrophobic surfaces, both smooth and having high surface roughness of varying length scales (to generate superhydrophobicity), were incubated in protein solution. The samples were then exposed to flow shear in a device designed to simulate a microfluidic environment. They reported a similar amount of protein adsorbed onto smooth and nanometer-scale rough surfaces with static incubation, although a greater amount was found to adsorb onto superhydrophobic surfaces with micrometer scale roughness resulted from the increasing binding strength of hydrophobic interactions between Bovine

serum albumin and the superhydrophobic surface. However, incubated in a flow cell similar to that used in microfluidics, flow shear removed a considerably larger proportion of adsorbed protein from the superhydrophobic surfaces than from the smooth ones, with almost all of the protein being removed from some nanoscaled surfaces. This type of surface may therefore be useful in microfluidics, where protein sticking is a problem. Moreover, they reported that superhydrophobic surfaces with larger roughness dimensions (~4 μm or 800 nm particle size) caused increased adsorption of protein than the copper oxide nano-pillars about 60 nm wide and 10 nm thick.

Platelet adhesion and activation on biomedical material surfaces may result in blood coagulation and thrombosis. Therefore, regulating the wettability to increase the blood-compatibility is an efficient way for platelet anti-adhesion. Sun et al. reported a kind of blood-compatible superhydrophobic surface constructed by dip-coating fluorinated poly(carbonate urethane) onto aligned carbon nanotubes.[142] Compared to ordinary smooth film, the as-prepared superhydrophobic structured film can greatly decrease the adhesion and activation of platelet. This indicates that the special topography and wettability play critical role in blood-compatibility. Recently, we studied a kind of anti-platelet and UV light responsive surface, based on low surface energy materials self-assembly on vertical aligned TiO_2 nanotube arrays.[143] The *in vitro* blood compatibility experimental indicated that the superhydrophobic nanotube TiO_2 layers with low solid–liquid adhesion exhibit a remarkable resistance to platelets attachment (Figs. 13(a, b)). Compared to the relatively high amount of platelets on superhydrophilic TiO_2 nanotube layers (22 ± 1.5 per 5000 μm^2), only very few platelets (1 ± 0.8 per 5000 μm^2) were found to adhere on the superhydrophobic TiO_2 nanotube layers. Moreover, even though some platelets were occasionally attached on the superhydrophobic surface, they looked smooth without any growth of pseudopods (inset), implying that the platelets adhered on the superhydrophobic TiO_2 nanotube surface remain inactive and hardly grow and spread out. From the *in vitro* evaluation, the superhydrophobic TiO_2 nanotube layers exhibited excellent blood compatibility and remarkable performance in preventing platelets from adhering to the implant surface. Furthermore, patterned superhydrophobic films exhibit excellent anti-adhesion performance by cells.[144, 145] The *in vitro* MG-63 cell tests of the micropatterned octacalcium phosphate (OCP) on superhydrophobic TiO_2 nanotube array films demonstrated that the cells had selective adhesion on the tiny square units of OCP films (Figs. 13(c, d)), which is promising for controlling the adherent growth of the cells on the tiny units. This would enable high throughput evaluation of the cell behaviors and other related applications.

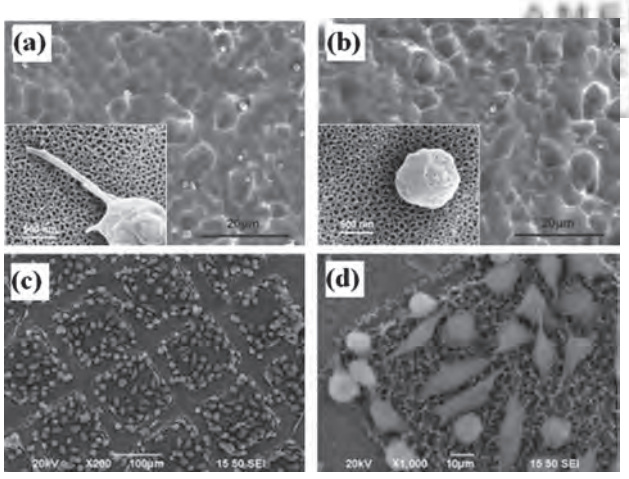

Fig. 13. SEM images of adhered platelets on superhydrophilic surface (a) and superhydrophobic surface (b) at 37 °C for 120 min. Reprinted with permission from Ref. [143], Y. Yang et al., *Colloids Surf. B* 79, 309 **(2010)**. © 2010, Elsevier. The insets are the corresponding magnified images. (c, d) SEM micrographs of MG-63 cells cultured on the patterned OCP coatings for 6 h. Low magnification (c) and high magnification of (d). Reprinted with permission from Ref. [144], Y. X. Huang et al., *Acta Phys.-Chim. Sin.* 26, 2057 **(2010)**. © 2010, Chinese Chemical Society.

3.7. Micro-Template for Patterning

Uniform assembly of functional inorganic nanomaterials remains a primary challenge. Nature adopts a superior approach in biomineralization, where "matrix" macromolecules induce nucleation of inorganic crystals at specific locations with controlled size and morphology, and sometimes even with defined growth orientation. Recently, patterned thin films had received considerable attention due to their interesting properties for widely potential applications, such as opto-electronic devices, magnetic storage media, optical and gas sensor, microfluidic system.[151–155] Comparing to the conventional patterning technique such as physical vapor deposition, chemical vapor deposition and sputtering, solution-based deposition method are becoming popular for the fabrication of patterning films due to the low temperature process under ambient environment, less energy and time consumption, and facile control of the experimental parameters.[156–159] Although the common photolithographic technique is excellent for preparing submicron-sized template for patterning in solution, it is a complex multi-step process that has to remove great part of the formed film and the supplemental photoresist.[160] Superhydrophilic/superhydrophobic wetting pattern with an extreme wettability contrast by photolithography, particular the rewritable pattern by using high photocatalytic active TiO_2 structure surfaces,[161–165] is a potentially powerful and economical approach to precisely construct functional nanostructures in aqueous solution.[166–170]

On the basis of photolithography patterning technique on TiO_2 structures, we applied the as-prepared

REVIEW

superhydrophilic–superhydrophobic pattern to direct and guide the selective etching of TiO_2 nanotubes (Figure 14(a, b)) or deposition of ZnO nanorods onto the TiO_2 nanotube film (Figs. 13(c, d)).[171, 172] It can be clearly seen that TiO_2 nanotube are preferred to be etched by HF vapor within the superhydrophilic regions to form negative pattern while the superhydrophobic areas are kept intact. In the case of the electrodeposition, ZnO nanorods are preferentially deposited on superhydrophilic regions to generate positive pattern (Figs. 14(c, d)). On the center of the superhydrophobic region, micro-concaves (indicated by the arrows) resulted from anisotropic etching of the underlying Ti grains can still be seen on the substrate due to the uncovering of ZnO nanorod crystals. This is ascribed to the superhydrophobic regions that are able to keep away any aqueous solution with the help of air trapped in the liquid/solid interface. Following this principle, arrays of crystalline CdS materials,[173] silver nanoparticles[174] and OCP biomaterials[175] were nucleated and assembled directly from solution onto Ti substrates at the desired locations precisely. These patterned structures can then be fabricated into arrays of photodetector, matrix devices for large-area microelectronic applications or bio-compatible coatings where drugs could be encapsulated in specific areas of the coating.[176] This strategy of micropatterned nanocomposites will be helpful to develop various micropatterned functional nanostructured materials. However, a grand challenge for wide-spread practical applications remains to be the development of high-throughput, low-cost, and easily-controlled techniques to achieve desired orientation and order of the nano-blocks.

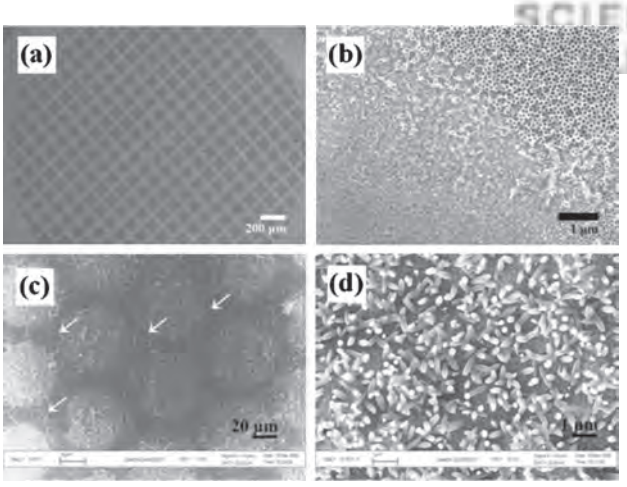

Fig. 14. Typical SEM image of the selectively etching of TiO_2 nanotube arrays (a, b) Reprinted with permission from Ref. [171], Y. K. Lai et al., *J. Electrochem. Soc.* 156, D480 **(2009)**. © 2009, The Electrochemical Society, and ZnO nanorod films (c, d) deposition in predefined superhydrophilic regions on TiO_2 nanotube films by electrochemical deposition. Reprinted with permission from Ref. [172], Y. K. Lai et al., *New J. Chem.* 34, 44 **(2010)**. © 2010, The Royal Society of Chemistry.

3.8. Friction Reduction

The transport of a liquid through a conventional smooth pipe or tube is dominated by the frictional drag on the liquid against the walls. Usually, a layer of gas at or near the boundary between the solid and liquid, achieved by the vaporization of liquid, by a cushion of air (e.g., below a hovercraft), or by producing bubbles at the interface, can reduce the resistance to flow against a solid. However, these methods require a continuous energy input. Recently, nonstick superhydrophobic surfaces demonstrating high apparent contact angles, low contact area and lateral friction to liquid droplets on natural and artificial surfaces have attracted much attention of researchers.[177–186] Watanable and Zou et al. reported a reduced flow adhesion and friction phenomena when water passed through superhydrophobic surface, with a comparison to lower anti-wetting surfaces.[177, 178] The reduction of liquid flow resistance is ascribed to the reduced molecular attraction and the resultant liquid–solid contact area by the air layer trapped in the rough micro- and nanostructured superhydrophobic surfaces. Bizonne et al. also confirmed the reduction of lateral friction on superhydrophobic structure surfaces through experimental and numerical simulation.[179] To our knowledge, most reported research used small sections of lithographically patterned surfaces and rarely considered the pressure differences or varying flow rates. McHale et al. observed that the superhydrophobic nanoribbon coating allowed greater flow at low pressure differences, but the effect on friction reduction disappeared as the pressure increased.[180] Large pressure and friction forces are known to be detrimental in micro-electro-mechanical system (MEMS) applications due to large surface-to-volume ratio and minute spacing between structures in MEMS.[181, 182] Carlborg et al.

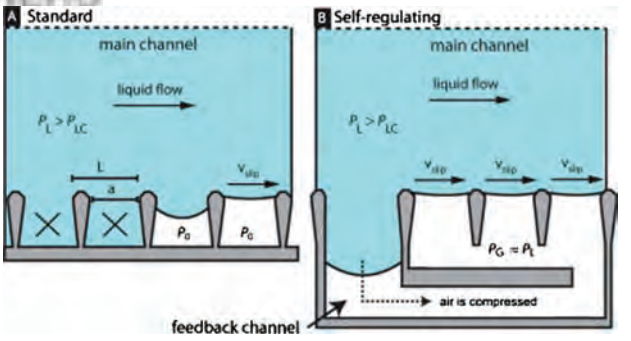

Fig. 15. Standard and self-regulating air pressure on superhydrophobic structure surface. (A) In a standard superhydrophobic surface, the gas pockets remain at the same air pressure (atmospheric) and collapse when the liquid pressure is too high. (B) In the self-regulating design, the gas-pocket pressure is pneumatically connected to the liquid via a feedback channel. When liquid enters the feedback channel, the air is compressed, and the pressure drop over the gas–liquid interface is reduced. Reprinted with permission from Ref. [186], C. F. Carlborg and W. van der Wijngaart, *Langmuir* 27, 487 **(2011)**. © 2011, American Chemistry Society.

reported a novel self-regulating technique for reducing the friction losses in large microchannels at high liquid pressures and large liquid flows, which can overcome previous limitations with regard to sustainable liquid pressure on a superhydrophobic surface (Fig. 15).[186] Their design of the superhydrophobic channel can automatically adjust the gas pressure in the lubricating air layer to the local liquid pressure in the channel by pneumatically connecting the liquid in the microchannel to the gas-pockets trapped at the channel wall through a pressure feedback channel. When liquid enters the feedback channel, it compresses the air and increases the pressure in the gas-pocket. This technique reduces the pressure drop over the gas–liquid interface and achieves sustained superhydrophobic friction reduction under high liquid pressures and large flows.

4. SUMMARY AND OUTLOOK

The present article reviews the recent progress on the natural and bio-inspired superhydrophobic surfaces with different types of adhesion property, such as low adhesion, high adhesion, anisotropic adhesion, and stimuli-responsive adhesion. Studies on the biological structure surfaces and the mimetic fabrication of bio-inspired synthetic surfaces reveal that the combination of topography structure and chemical component results in these special adhesion states. For example, the tailoring of topography and the scale of micro- and nanostructures to achieve certain contact models can effectively change the solid–liquid adhesion from low to high levels. On the other hand, the special arrangement of the micro-structures and the chemical component may result in anisotropic solid–liquid adhesion. Furthermore, reversible switching of adhesion between the low-adhesive rolling state and high-adhesive pinning state for a water droplet on a superhydrophobic surface could be achieved via cooperation of the stimuli-responsive materials and surface roughness. In addition, potential applications of superhydrophobic surfaces with special adhesion were also discussed, including self-cleaning, water/oil separation, microfluidic manipulation and micro-templates.

Superhydrophobic surface with responsive liquid adhesion have attracted much attention, great progress has been made in recent years. However, up to now, most adhesion changes reported are achieved *ex-situ*, which require a different droplet to study the adhesion on the smart responsive surface. Many problems, such as stability and cost of materials with multi-functionalities need to be addressed before industrial applications can be realized. Therefore, renewable, stable and smart responsive superhydrophobic surface with solid–liquid adhesion changing in a high contrast under single or multiple stimuli-responses is a key issue for future investigation. Moreover, the *in-situ* and fast adhesive force measurement on the superhydrophobic is still need to be improved.

Acknowledgments: The authors thank the National Natural Science Foundation of China (grants 51072170, 20773100, 21021002), the National Basic Research Program of China (grant 2007CB935603) and the National High Technology Research and Development Program of China (grant 2009AA03Z327), and the Environment and Water Industry Programme Office (EWI) under the National Research Foundation of Singapore (grant MEWR651/06/160) for their financial supports.

References and Notes

1. A. Nakajima, A. Fujishima, K. Hashimoto, and T. Watanabe, *Adv. Mater.* 11, 1365 (**1999**).
2. L. Feng, S. H. Li, Y. S. Li, H. J. Li, L. J. Zhang, J. Zhai, Y. L. Song, B. Q. Liu, L. Jiang, and D. B. Zhu, *Adv. Mater.* 14, 1857 (**2002**).
3. A. Lafuma and D. Quéré, *Nat. Mater.* 2, 457 (**2003**).
4. T. L. Sun, L. Feng, X. F. Gao, and L. Jiang, *Acc. Chem. Res.* 38, 644 (**2005**).
5. X. J. Feng and L. Jiang, *Adv. Mater.* 18, 3063 (**2006**).
6. M. L. Ma and R. M. Hill, *Curr. Opin. Colloid Interface Sci.* 11, 193 (**2006**).
7. N. Zhao, X. Y. Lu, X. Y. Zhang, H. Y. Liu, S. X. Tan, and J. Xu, *Prog. Chem.* 19, 860 (**2007**).
8. D. Quéré, *Ann. Rev. Mater. Res.* 38, 71 (**2008**).
9. P. Roach, N. J. Shirtcliffe, and M. I. Newton, *Soft Matter* 4, 224 (**2008**).
10. F. Xia and L. Jiang, *Adv. Mater.* 20, 2842 (**2008**).
11. C. Dorrer and J. Ruhe, *Soft Matter* 5, 51 (**2009**).
12. J. X. Wang, Y. Z. Zhang, T. Y. Zhao, Y. L. Song, and L. Jiang, *Sci. China-Chem.* 53, 318 (**2010**).
13. M. Kamperman, E. Kroner, A. del Campo, R. M. McMeeking, and E. Arzt, *Adv. Eng. Mater.* 12, 335 (**2010**).
14. K. S. Liu, X. Yao, and L. Jiang, *Chem. Soc. Rev.* 39, 3240 (**2010**).
15. B. W. Xin and J. C. Hao, *Chem. Soc. Rev.* 39, 769 (**2010**).
16. X. M. Li, D. Reinhoudt, and M. Crego-Calama, *Chem. Soc. Rev.* 36, 1350 (**2007**).
17. A. del Campo and E. Arzt, *Chem. Rev.* 108, 911 (**2008**).
18. X. Zhang, F. Shi, J. Niu, Y. G. Jiang, and Z. Q. Wang, *J. Mater. Chem.* 18, 621 (**2008**).
19. M. J. Liu, Y. M. Zheng, J. Zhai, and L. Jiang, *Acc. Chem. Res.* 43, 368 (**2010**).
20. M. J. Liu and L. Jiang, *Adv. Funct. Mater.* 20, 3753 (**2010**).
21. C. R. Crick and I. P. Parkin, *Chem.-Eur. J.* 16, 3568 (**2010**).
22. Z. G. Guo, W. M. Liu, and B. L. Su, *J. Colloid Interface Sci.* 353, 335 (**2011**).
23. B. Bhushan and Y. C. Jung, *Prog. Mater. Sci.* 56, 1 (**2011**).
24. X. Yao, Y. L. Song, and L. Jiang, *Adv. Mater.* 23, 719 (**2011**).
25. A. B. D. Cassie and S. Baxter, *Trans. Faraday Soc.* 40, 546 (**1944**).
26. R. N. Wenzel, *Ind. Eng. Chem.* 28, 988 (**1936**).
27. S. Wang and L. Jiang, *Adv. Mater.* 19, 3423 (**2007**).
28. G. McHale, N. J. Shirtcliffe, and M. I. Newton, *Langmuir* 20, 10146 (**2004**).
29. J. F. Zhang and D. Y. Kwok, *Langmuir* 22, 4998 (**2006**).
30. H. Kusumaatmaja, and J. M. Yeomans, *Langmuir* 23, 6019 (**2007**).
31. M. H. Jin, X. J. Feng, L. Feng, T. L. Sun, J. Zhai, T. J. Li, and L. Jiang, *Adv. Mater.* 17, 1977 (**2005**).
32. K. S. Liu, M. L. Zhang, J. Zhai, J. Wang, and L. Jiang, *Appl. Phys. Lett.* 92, 183103 (**2008**).
33. X. F. Gao and L. Jiang, *Nature* 432, 36 (**2004**).
34. X. Q. Feng, X. F. Gao, Z. N. Wu, L. Jiang, and Q. S. Zheng, *Langmuir* 23, 4892 (**2007**).

REVIEW

35. Z. G. Guo, F. Zhou, J. C. Hao, and W. M. Liu, *J. Am. Chem. Soc.* 127, 15670 (**2005**).
36. W. C. Wu, X. L. Wang, D. A. Wang, M. Chen, F. Zhou, W. M. Liu, and Q. J. Xue, *Chem. Commun.* 9, 1043 (**2009**).
37. X. Yao, Q. W. Chen, L. Xu, Q. K. Li, Y. L. Song, X. F. Gao, D. Quéré, and L. Jiang, *Adv. Funct. Mater.* 20, 656 (**2010**).
38. X. F. Wu and G. Q. Shi, *J. Phys. Chem. B* 110, 11247 (**2006**).
39. B. Bhushan, K. Koch, and Y. C. Jung, *Soft Matter* 4, 1799 (**2008**).
40. B. Bhushan, Y. C. Jung, A. Niemietz, and K. Koch, *Langmuir* 25, 1659 (**2009**).
41. K. Koch, B. Bhushan, Y. C. Jung, and W. Barthlott, *Soft Matter* 5, 1386 (**2009**).
42. M. H. Jin, X. J. Feng, J. M. Xi, J. Zhai, K. W. Cho, L. Feng, and L. Jiang, *Macromol. Rapid Commun.* 26, 1805 (**2005**).
43. M. Nosonovsky and B. Bhushan, *Curr. Opin. Colloid Interface Sci.* 14, 270 (**2009**).
44. W. Ma, M. H. Jin, C. L. Yu, M. Y. Liao, and Y. Zhao, *Chem. J. Chinese U* 10, 2096 (**2009**).
45. A. Tuteja, W. Choi, M. L. Ma, J. M. Mabry, S. A. Mazzella, G. C. Rutledge, G. H. McKinley, and R. E. Cohen, *Science* 318, 1618 (**2007**).
46. Q. D. Xie, J. Xu, L. Feng, L. Jiang, W. H. Tang, X. D. Luo, and C. C. Han, *Adv. Mater.* 16, 302 (**2004**).
47. J. M. Xi, L. Feng, and L. Jiang, *Appl. Phys. Lett.* 92, 053102 (**2008**).
48. H. F. Meng, S. T. Wang, J. M. Xi, Z. Y. Tang, and L. Jiang, *J. Phys. Chem. C* 112, 11454 (**2008**).
49. D. A. Wang, X. L. Wang, X. J. Liu, and F. Zhou, *J. Phys. Chem. C* 114, 9938 (**2010**).
50. L. Feng, Y. A. Zhang, J. M. Xi, Y. Zhu, N. Wang, F. Xia, and L. Jiang, *Langmuir* 24, 4114 (**2008**).
51. B. Bhushan and E. K. Her, *Langmuir* 26, 8207 (**2010**).
52. K. Autumn, Y. A. Liang, S. T. Hsieh, W. Zesch, W. P. Chan, T. W. Kenny, R. Fearing, and R. J. Full, *Nature* 405, 681 (**2000**).
53. K. Autumn, M. Sitti, Y. A. Liang, A. M. Peattie, W. R. Hansen, S. Sponberg, T. W. Kenny, R. Fearing, J. N. Israelachvili, and R. J. Full, *Proc. Natl. Acad. Sci. USA* 99, 12252 (**2002**).
54. Z. G. Guo and W. M. Liu, *Appl. Phys. Lett.* 90, 223111 (**2007**).
55. N. D. Boscher, C. J. Carmalt, and I. P. Parkin, *J. Mater. Chem.* 16, 122 (**2006**).
56. W. L. Yu, T. J. Yao, X. A. Li, T. Q. Wang, H. N. Gao, J. H. Zhang, and B. Yang, *J. Appl. Polymer. Sci.* 119, 1052 (**2011**).
57. W. J. Zhao, L. P. Wang, and Q. J. Xue, *J. Phys. Chem. C* 114, 11509 (**2010**).
58. Y. K Lai, Y. C. Chen, Y. X. Tang, D. G. Gong, Z. Chen, and C. J. Lin, *Electrochem. Commun.* 11, 2268 (**2009**).
59. S. G. Park, H. H. Moon, S. K. Lee, J. Shim, and S. M. Yang, *Langmuir* 26, 1468 (**2010**).
60. S. J. Zhu, Y. F. Li, J. H. Zhang, C. L. Lu, X. Dai, F. Jia, H. N. Gao, and B. Yang, *J. Colloid Interface Sci.* 344, 541 (**2010**).
61. Y. K. Lai, X. F. Gao, H. F. Zhuang, J. Y. Huang, C. J. Lin, and L. Jiang, *Adv. Mater.* 21, 3799 (**2009**).
62. B. G. Park, W. Lee, J. S. Kim, and K. B. Lee, *Colloids Surf. A* 370, 15 (**2010**).
63. W. Lee, B. G. Park, D. H. Kim, D. J. Ahn, Y. Park, S. H. Lee, and K. B. Lee, *Langmuir* 26, 1412 (**2010**).
64. Z. J. Cheng, J. Gao, and L. Jiang, *Langmuir* 26, 8233 (**2010**).
65. B. Balu, J. S. Kim, V. Breedveld, and D. W. Hess, *J. Adhesion Sci. Technol.* 23, 361 (**2009**).
66. R. Di Mundo, F. Palumbo, and R. d'Agostino, *Langmuir* 24, 5044 (**2008**).
67. X. Y. Song, J. Zhai, Y. L. Wang, and L. Jiang, *J. Phys. Chem. B* 109, 4048 (**2005**).
68. L. C. Gao, T. J. McCarthy, and X. Zhang, *Langmuir* 25, 14100 (**2009**).
69. J. L. Zhang and Y. C. Han, *Langmuir* 24, 796 (**2008**).
70. W. H. Ting, C. C. Chen, S. A. Dai, S. Y. Suen, I. K. Yang, L. Liu, F. M. C. Chen, and R. J. Jeng, *J. Mater. Chem.* 19, 4819 (**2009**).
71. X. Y. Song, J. Zhai, Y. L. Wang, and L. Jiang, *J. Phys. Chem. B* 109, 4048 (**2005**).
72. Y. K. Lai, C. J. Lin, J. Y. Huang, H. F. Zhuang, L. Sun, and T. Nguyen, *Langmuir* 24, 3867 (**2008**).
73. R. Di Mundo, F. Palumbo, and R. d'Agostino, *Langmuir* 26, 5196 (**2010**).
74. W. Sun, L. Y. Shen, L. M. Wang, K. Fu, and J. Ji, *Langmuir* 26, 14236 (**2010**).
75. J. Yang, Z. Z. Zhang, X. H. Men, X. H. Xu, and X. T. Zhu, *J. Colloid Interface Sci.* 346, 241 (**2010**).
76. J. Y. Peng, P. R. Yu, S. J. Zeng, X. Liu, J. R. Chen, and W. J. Xu, *J. Phys. Chem. C* 114, 5926 (**2010**).
77. N. Zhao, Q. D. Xie, X. Kuang, S. Q. Wang, Y. F. Li, X. Y. Lu, S. X. Tan, J. Shen, X. L. Zhang, Y. J. Zhang, J. Xu, and C. C. Han, *Adv. Funct. Mater.* 17, 2739 (**2007**).
78. X. J. Liu, Q. Ye, B. Yu, Y. M. Liang, W. M. Liu, and F. Zhou, *Langmuir* 26, 12377 (**2010**).
79. D. A. Wang, Y. Liu, X. J. Liu, F. Zhou, W. M. Liu, and Q. J. Xue, *Chem. Commun.* 45, 7018 (**2009**).
80. X. J. Liu, W. C. Wu, X. L. Wang, Z. Z. Luo, Y. M. Liang and F. Zhou, *Soft Matter* 5, 3097 (**2009**).
81. X. J. Liu, M. R. Cai, Y. M. Liang, F. Zhou, and W. M. Liu, *Soft Matter* 7, 3331 (**2011**).
82. X. T. Zhu, Z. Z. Zhang, X. H. Men, J. Yang, and X. H. Xu, *Appl. Surf. Sci.* 256, 7619 (**2010**).
83. K. Uchida, N. Nishikawa, N. Izumi, S. Yamazoe, H. Mayama, Y. Kojima, S. Yokojima, S. Nakamura, K. Tsujii, and M. Irie, *Angew. Chem. Int. Ed.* 49, 5942 (**2010**).
84. T. N. Krupenkin, J. A. Taylor, T. M. Schneider, and S. Yang, *Langmuir* 20, 3824 (**2004**).
85. X. D. Zhao, H. M. Fan, J. Luo, J. Ding, X. Y. Liu, B. S. Zou, and Y. P. Feng, *Adv. Funct. Mater.* 21, 184 (**2011**).
86. M. J. Liu, F. Q. Nie, Z. X. Wei, Y. L. Song, and L. Jiang, *Langmuir* 26, 3993 (**2010**).
87. N. Verplanck, E. Galopin, J. C. Camart, V. Thomy, Y. Coffinier, and R. Boukherroub, *Nano Lett.* 7, 813 (**2007**).
88. F. Lapierre, V. Thomy, Y. Coffinier, R. Blossey, and R. Boukherroub, *Langmuir* 25, 6551 (**2009**).
89. C. Li, R. W. Guo, X. Jiang, S. X. Hu, L. Li, X. Y. Cao, H. Yang, Y. L. Song, Y. M. Ma, and L. Jiang, *Adv. Mater.* 21, 4254 (**2009**).
90. L. Chen, M. J. Liu, L. Lin, T. Zhang, J. Ma, Y. L. Song, and L. Jiang, *Soft Matter* 6, 2708 (**2010**).
91. X. Hong, X. Gao, and L. Jiang, *J. Am. Chem. Soc.* 129, 1478 (**2007**).
92. Z. J. Cheng, L. Feng, and L. Jiang, *Adv. Funct. Mater.* 18, 3219 (**2008**).
93. D. Wu, S. Z. Wu, Q. D. Chen, Y. L. Zhang, J. Yao, X. Yao, L. G. Niu, J. N. Wang, L. Jiang, and H. B. Sun, *Adv. Mater.* 23, 545 (**2011**).
94. J. L. Zhang, X. Y. Lu, W. H. Huang, and Y. C. Han, *Macromol. Rapid Commun.* 26, 477 (**2005**).
95. Q. L. Zhang, F. Xia, T. L. Sun, W. L. Song, T. Y. Zhao, M. C. Liu, and L. Jiang, *Chem. Commun.* 10, 1199 (**2008**).
96. D. Tian, Q. Chen, F. Q. Nie, J. J. Xu, Y. L. Song, and L. Jiang, *Adv. Mater.* 21, 3744 (**2009**).
97. F. Xia, H. Ge, Y. Hou, T. L. Sun, L. Chen, G. Z. Zhang, and L. Jiang, *Adv. Mater.* 19, 2520 (**2007**).
98. D. A. Wang, X. L. Wang, X. J. Liu, and F. Zhou, *J. Phys. Chem. C* 114, 9938 (**2010**).
99. X. X. Chen, J. Gao, B. Song, M. Smet, and X. Zhang, *Langmuir* 26, 104 (**2010**).
100. Y. Chen, B. He, J. H. Lee, and N. A. Patankar, *J. Colloid Interface Sci.* 281, 458 (**2005**).
101. X. F. Gao, X. Yao, and L. Jiang, *Langmuir* 23, 4886 (**2007**).

102. Y. M. Zheng, X. F. Gao, and L. Jiang, *Soft Matter* 3, 178 **(2007)**.
103. N. A. Malvadkar, M. J. Hancock, K. Sekeroglu, W. J. Dressick, and M. C. Demirel, *Nat. Mater.* 9, 1023 **(2010)**.
104. H. Kusumaatmaja and J. M. Yeomans, *Soft Matter* 5, 2704 **(2009)**.
105. W. Barthlott and C. Neinhuis, *Planta* 202, 1 **(1997)**.
106. R. Furstner, W. Barthlott, C. Neinhuis, and P. Walzel, *Langmuir* 21, 956 **(2005)**.
107. A. Nakajima, K. Hashimoto, T. Watanabe, K. Takai, G. Yamauchi, and A. Fujishima, *Langmuir* 16, 7044 **(2000)**.
108. B. Bhushan, Y. C. Jung, and K. Koch, *Langmuir* 25, 3240 **(2009)**.
109. D. P. Qi, N. Lu, H. B. Xu, B. J. Yang, C. Y. Huang, M. J. Xu, L. G. Gao, Z. X. Wang, and L. F. Chi, *Langmuir* 25, 7769 **(2009)**.
110. D. Nystrom, J. Lindqvist, E. Ostmark, P. Antoni, A. Carlmark, A. Hult, and E. Malmstrom, *ACS Appl. Mater. Interface* 1, 816 **(2009)**.
111. Y. H. Xiu, D. W. Hess, and C. P. Wong, *J. Adhes. Sci. Technol.* 22, 1907 **(2008)**.
112. L. Mishchenko, B. Hatton, V. Bahadur, J. A. Taylor, T. Krupenkin, and J. Aizenberg, *ACS Nano* 4, 7699 **(2010)**.
113. S. A. Kulinich, S. Farhadi, K. Nose, and X. W. Du, *Langmuir* 27, 25 **(2011)**.
114. L. L. Cao, A. K. Jones, V. K. Sikka, J. Z. Wu, and D. Gao, *Langmuir* 25, 12444 **(2009)**.
115. Z. L. Liu, Y. J. Gou, J. T. Wang, and S. Y. Cheng, *Int. J. Heat Mass. Tran.* 51, 5975 **(2008)**.
116. X. F. Gao, X. Yan, X. Yao, L. Xu, K. Zhang, J. H. Zhang, B. Yang, and L. Jiang, *Adv. Mater.* 19, 2213 **(2007)**.
117. J. H. Zhang and B. Yang, *Adv. Funct. Mater.* 20, 3411 **(2010)**.
118. M. He, J. X. Wang, H. L. Li, X. L. Jin, J. J. Wang, B. Q. Liu, and Y. L. Song, *Soft Matter* 6, 2396 **(2010)**.
119. M. He, J. X. Wang, H. L. Li, and Y. L. Song, *Soft Matter* 7, 3993 **(2011)**.
120. S. Jung, M. Dorrestijn, D. Raps, A. Das, C. M. Megaridis, and D. Poulikakos, *Langmuir* 27, 3059 **(2011)**.
121. A. J. Meuler, J. D. Smith, K. K. Varanasi, J. M. Mabry, G. H. McKinley, and R. E. Cohen, *ACS Appl. Mater. Interface* 2, 3100 **(2010)**.
122. B. Balu, A. D. Berry, D. W. Hess, and V. Breedveld, *Lab Chip* 9, 3066 **(2009)**.
123. L. T. Shi, C. G. Jiang, G. J. Ma, and C. W. Wu, *Biomicrofluidics* 4, 041101 **(2010)**.
124. A. Chunder, K. Etcheverry, G. Longde, H. J. Cho, and L. Zhai, *Colloids Surf. A* 333, 187 **(2009)**.
125. E. Bormashenko, R. Pogreb, Y. Bormashenko, A. Musin, and T. Stein, *Langmuir* 24, 12119 **(2008)**.
126. Y. Zhao, J. Fang, H. X. Wang, X. G. Wang, and T. Lin, *Adv. Mater.* 22, 707 **(2010)**.
127. Y. M. Zheng, H. Bai, Z. B. Huang, X. L. Tian, F. Q. Nie, Y. Zhao, J. Zhai, and L. Jiang, *Nature* 463, 640 **(2010)**.
128. H. Bai, X. L. Tian, Y. M. Zheng, J. Ju, Y. Zhao, and L. Jiang, *Adv. Mater.* 22, 5521 **(2010)**.
129. N. J. Shirtcliffe, G. McHale, and M. I. Newton *Langmuir* 25, 14121 **(2009)**.
130. A. R. Parker and C. R. Lawrence, *Nature* 414, 33 **(2001)**.
131. L. Zhai, M. C. Berg, F. C. Cebeci, Y. Kim, J. M. Milwid, M. F. Rubner, and R. E. Cohen, *Nano Lett.* 6, 1213 **(2006)**.
132. C. Dorrer and J. Ruhe, *Langmuir* 24, 6154 **(2008)**.
133. R. P. Garrod, L. G. Harris, W. C. E. Schofield, J. McGettrick, L. J. Ward, D. O. H. Teare, and J. P. S. Badyal, *Langmuir* 23, 689 **(2007)**.
134. C. H. Lee, N. Johnson, J. Drelich, and Y. K. Yap, *Carbon* 49, 669 **(2011)**.
135. H. L. Li, J. X. Wang, L. M. Yang, and Y. L. Song, *Adv. Funct. Mater.* 18, 3258 **(2008)**.
136. Q. Zhu, F. Tao, and Q. M. Pan, *ACS Appl. Mater. Interfaces* 1, 3141 **(2010)**.
137. L. Feng, Z. Y. Zhang, Z. H. Mai, Y. M. Ma, B. Q. Liu, L. Jiang, and D. B. Zhu, *Angew. Chem. Int. Ed.* 43, 2012 **(2004)**.
138. J. L. Zhang, W. H. Huang, and Y. C. Han, *Macromol. Rapid Comm.* 27, 804 **(2006)**.
139. J. K. Yuan, X. G. Liu, O. Akbulut, J. Q. Hu, S. L. Suib, J. Kong, and F. Stellacci, *Nat. Nanotechnol.* 3, 332 **(2008)**.
140. X. C. Gui, J. Q. Wei, K. L. Wang, A. Y. Cao, H. W. Zhu, Y. Jia, Q. Shu, and D. H. Wu, *Adv. Mater.* 22, 617 **(2010)**.
141. Y. Koc, A. J. de Mello, G. McHale, M. I. Newton, P. Roach, and N. J. Shirtcliffe, *Lab Chip* 8, 582 **(2008)**.
142. T. L. Sun, H. Tan, D. Han, Q. Fu, and L. Jiang, *Small* 1, 959 **(2005)**.
143. Y. Yang, Y. K. Lai, Q. Q. Zhang, K. Wu, L. H. Zhang, C. J. Lin, and P. F. Tang, *Colloids Surf. B* 79, 309 **(2010)**.
144. Y. X. Huang, Y. K. Lai, L. X. Lin, L. Sun, and C. J. Lin, *Acta Phys.-Chim. Sin.* 26, 2057 **(2010)**.
145. T. Ishizaki, N. Saito, and O. Takai, *Langmuir* 26, 8147 **(2010)**.
146. L. Chen, M. J. Liu, H. Bai, P. P. Chen, F. Xia, D. Han, and L. Jiang, *J. Am. Chem. Soc.* 131, 10467 **(2009)**.
147. J. Genzer and K. Efimenko, *Biofouling* 22, 339 **(2006)**.
148. M. Zhou, J. H. Yang, X. Ye, A. R. Zheng, G. Li, P. F. Yang, Y. Zhu, and L. Cai, *J. Nano Res.* 2, 129 **(2008)**.
149. C. Mao, C. X. Liang, W. P. Luo, J. C. Bao, J. Shen, X. M. Hou, and W. B. Zhao, *J. Mater. Chem.* 19, 9025 **(2009)**.
150. X. M. Hou, X. B. Wng, Q. S. Zhu, J. C. Bao, C. Mao, L. C. Jiang, and J. A. Shen, *Colloids Surf. B* 80, 247 **(2010)**.
151. R. A. Segalman, *Mater. Sci. Eng. R* 48, 191 **(2005)**.
152. F. F. Amos, S. A. Morin, J. A. Streifer, R. J. Hamers, and S. Jin, *J. Am. Chem. Soc.* 129, 14296 **(2007)**.
153. P. Mitra, A. P. Chatterjee, and H. S. Maiti, *Mater. Lett.* 35, 33 **(1998)**.
154. M. H. Huang, S. Mao, H. Feick, H. Q. Yan, Y. Y. Wu, H. Kind, E. Weber, R. Russo, and P. D. Yang, *Science* 292, 1897 **(2001)**.
155. N. Shirahata, W. Shin, N. Murayama, A. Hozumi, Y. Yokogawa, T. Kameyama, Y. Masuda, and K. Koumoto, *Adv. Funct. Mater.* 14, 580 **(2004)**.
156. Y. F. Gao, Y. Masuda, and K. Koumoto, *J. Nanosci. Nanotechnol.* 6, 1842 **(2006)**.
157. Y. Masuda, T. Sugiyama, and K. Koumoto, *J. Mater. Chem.* 12, 2643 **(2002)**.
158. M. Yoshimura and R. Gallage, *J. Solid State Electrochem.* 12, 775 **(2008)**.
159. S. H. Liu, W. C. M. Wang, S. C. B. Mannsfeld, J. Locklin, P. Erk, M. Gomez, F. Richter, and Z. N. Bao, *Langmuir* 23, 7428 **(2007)**.
160. A. Bessonov, J. G. Kim, J. W. Seo, J. W. Lee, and S. Lee, *Macromol. Chem. Phys.* 211, 2636 **(2010)**.
161. Y. K. Lai, L. Sun, Y. C. Chen, H. F. Zhuang, C. J. Lin, and J. W. Chin, *J. Electrochem. Soc.* 153, D123 **(2006)**.
162. H. F. Zhuang, C. J. Lin, Y. K. Lai, L. Sun, and J. Li, *Environ. Sci. Technol.* 41, 4735 **(2007)**.
163. Y. K. Lai, J. Y. Huang, H. F. Zhang, V. P. Subramaniam, Y. X. Tang, D. G. Gong, L. Sundar, L. Sun, Z. Chen, and C. J. Lin, *J. Hazard. Mater.* 184, 855 **(2010)**.
164. G. Caputo, C. Nobile, T. Kipp, L. Blasi, V. Grillo, E. Carlino, L. Manna, R. Cingolani, P. D. Cozzoli, and A. Athanassiou, *J. Phys. Chem. C* 112, 701 **(2008)**.
165. G. Caputo, R. Cingolani, P. D. Cozzoli, and A. Athanassiou, *Phys. Chem. Chem. Phys.* 11, 3692 **(2009)**.
166. A. Pittrof, S. Bauer, and P. Schmuki, *Acta Biomater.* 7, 424 **(2011)**.
167. Y. K. Lai, C. J. Lin, H. Wang, J. Y. Huang, H. F. Zhuang, and L. Sun, *Electrochem. Commun.* 10, 387 **(2008)**.
168. K. Nakata, S. Nishimoto, Y. Yuda, T. Ochiai, T. Murakami, and A. Fujishima, *Langmuir* 26, 11628 **(2010)**.
169. S. Nishimoto, H. Sekine, X. T. Zhang, Z. Y. Liu, K. Nakata, T. Murakami, Y. Koide, and A. Fujishima, *Langmuir* 25, 7226 **(2009)**.
170. H. Kinoshita, A. Ogasahara, Y. Fukuda, and N. Ohmae, *Carbon* 48, 4403 **(2010)**.
171. Y. K. Lai, J. Y. Huang, J. J. Gong, Y. X. Huang, C. L. Wang, Z. Chen, and C. J. Lin, *J. Electrochem. Soc.* 156, D480 **(2009)**.

REVIEW

172. Y. K. Lai, Z. Q. Lin, J. Y. Huang, L. Sun, Z. Chen, and C. J. Lin, *New J. Chem.* 34, 44 **(2010)**.
173. Y. K. Lai, Z. Q. Lin, Z. Chen, J. Y. Huang, and C. J. Lin, *Mater. Lett.* 64, 1309 **(2010)**.
174. Y. X. Huang, L. Sun, K. P. Xie, Y. K. Lai, B. J. Biu, B. Ren, and C. J. Lin, *J. Raman Spectrosc.* 42, 986 **(2011)**.
175. Y. K. Lai, Y. X. Huang, H. Wang, J. Y. Huang, Z. Chen, and C. J. Lin, *Colloids Surf. B* 76, 117 **(2010)**.
176. S. Bekou and D. Mattia, *Curr. Opin. Colloid Interface Sci.* DOI: 10.1016/j.cocis.2011.01.009 **(2011)**.
177. K. Watanabe, Y. Udagawa, and H. Udagawa, *J. Fluid Mech.* 381, 225 **(1999)**.
178. Y. Song, R. P. Nair, M. Zou, and Y. A. Wang, *Thin Solid Films* 518, 3801 **(2010)**.
179. C. Cottin-Bizonne, J. L. Barrat, L. Bocquet, and E. Charlaix, *Nat. Mater.* 2, 237 **(2003)**.
180. N. J. Shirtcliffe, G. MaHale, M. I. Newton, and Y. Zhang, *ACS Appl. Mater. Interface* 1, 1316 **(2009)**.
181. R. Maboudian and R. T. Howe, *J. Vac. Sci. Technol. B* 15, 1 **(1997)**.
182. K. Komvopoulos, *J. Adhes. Sci. Technol.* 17, 477 **(2003)**.
183. C. H. Choi and C. J. Kim, *Phys. Rev. Lett.* 96, 066001 **(2006)**.
184. A. M. J. Davis and E. Lauga, *J. Fluid Mech.* 661, 402 **(2010)**.
185. B. Su, M. Li, and Q. H. Lu, *Langmuir* 26, 6048 **(2010)**.
186. C. F. Carlborg and W. van der Wijngaart, *Langmuir* 27, 487 **(2011)**.

REVIEW